CrossMark

SHORT COMMUNICATION

Polymersomes mimic biofilms fractal growth

Alfredo Gonzalez-Perez[1,2,3] · Kasper Feld[3] · Juan M. Ruso[4]

Abstract We have mimicked the biofilm formation with highly stable biocompatible poly(2-methyl-2-oxazoline)-based polymersomes by simple spreading-drying of a droplet of the sample solution onto a glass support. The diffusion-limited aggregation process of polymersomes onto the surface was analyzed within a fractal framework. The different examples analyzed and presented together indicate one means by which the aggregation process can be controlled and predicted. The anti-bacterial adhesion properties of poly(2-methyl-2-oxazoline) allow potential uses in surface modification for biofouling prevention improving stability and response time.

Keywords Biofilms · fractals · polymersomes · AFM

Biofilms are a ubiquitous form of microbial colonization that profoundly affect human health via resistant infections and disrupt industrial processes generating costly problems through biofouling in power industry, shipping industry, water purification, pharmaceuticals, microelectronics and food industries [1, 2]. A noticeable effort has been paid to elucidate the mechanisms of biofilm formation and the mechanism that control bacterial cell adhesion [3], combining computational modeling and direct experiments in bacterial colonies [4, 5], by paying attention to the emergence of fractality.

Different methods for surface modification have been applied to control bacterial adhesion. In particular polymer brushes have been successfully used for antibacterial coating of sensitive surfaces by using the graft method [6]. Poly (ethylene oxide), PEO covalently attached to surfaces are commonly used for reducing bacterial adhesion [7]. The effect of critical parameters like the length of the polymer chain and the temperature in polyethylene oxide brushes can be tuned for optimal prevention of biofilm formation [8]. However, the low PEO stability has motivated research looking for new alternatives. In recent years poly (2-methyl-2-oxazoline) (PMOXA) have been found to show excellent antifouling properties with additional better stability properties. Besides, the PMOXA outperform PEO in protein-repellent properties in physiological and oxidative media [9–11].

In recent years block copolymers has become a new tool for the development of membrane-based soft materials [12–14]. In particular block copolymers are a promising alternative to develop biomimetic membranes by incorporation of functional membrane proteins or by direct chemical functionalization of the polymer blocks [15]. The incorporation of functional membrane proteins in pure block copolymer membranes is an emerging research area that promises to utilize the functionality of membrane proteins for industrial and biomedical uses. The use of highly stable supports, mechanically more robust than lipid membranes, was found advantageous. Several pioneering works demonstrated the feasibility of this approach in free standing membranes and vesicles [16, 17]. More recently a simplification of the membrane protein reconstitution protocols was achieved via self-direct

✉ Alfredo Gonzalez-Perez
 gonzalez@nbi.ku.dk; alfredo.gonzalez-perez@sydvatten.se

✉ Juan M. Ruso
  juanm.ruso@usc.es

1 Division of Water Resources Engineering, Lund University, P.O. Box 118, SE-22100 Lund, Sweden

2 Sweden Water Research AB, Ideon Science Park, Scheelevägen 15, SE-22370 Lund, Sweden

3 Membrane Biophysics Group, Niels Bohr Institute, University of Copenhagen, Blegdamsvej 17, 2100 Copenhagen, Denmark

4 Soft Matter and Molecular Biophysics Group, Department of Applied Physics, University of Santiago de Compostela, 15782 Santiago de Compostela, Spain
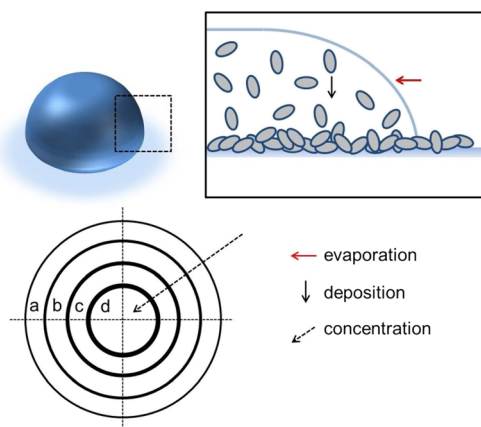
Fig. 1 Scheme of the deposition process via spreading-drying, showing the different droplet areas corresponding to different times, from the external circle to the internal one. The evaporation, deposition and polymersome concentration in bulk are time dependent. (Here "a" corresponds to time zero)

reconstitution [18]. Polymer functionalization allows, among others, the development of new biomedical applications. Lately, polymersomes with the adhesive properties of leukocites, leuko-polymersomes, have been developed with potential uses in theranostics [19–21]. In a previous work

using a triblock copolymer with a hydrophobic block based on poly(dimethylsiloxane) we demonstrated the functional reconstitution of gramicidin A on a large membrane area. Most recently we have investigated the formation of flat stable membranes into solid supports for surface functionalization [22, 23].

In the current work we used block copolymer-based vesicles, polymersomes, to mimic the biofilm formation on glass supports. The polymersome deposition was achieved by spreading and drying of a small drop of polymersome solution onto a glass support. The covering of the glass show a diffusion-limited aggregation process or DLA with fractal pattern analogous to those found in bacterial growth under starvation. The polymersomes form three dimensional clusters growing outside the surface similarly to the process of biofilm grow and maturation.

Polymersomes have been obtained at low concentration in aqueous solution using a triblock copolymer ($PMOXA_7$-$PDMS_{60}$-$PMOXA_7$) with molecular weight (MW) of 5800 g/mol, obtained from BioCure (USA) with 60 units of poly(dimethylsiloxane) (PDMS) and 7 units for the side blocks of poly(2-methyloxazoline) (PMOXA) carrying an additional methacrylate end groups. The sample preparation
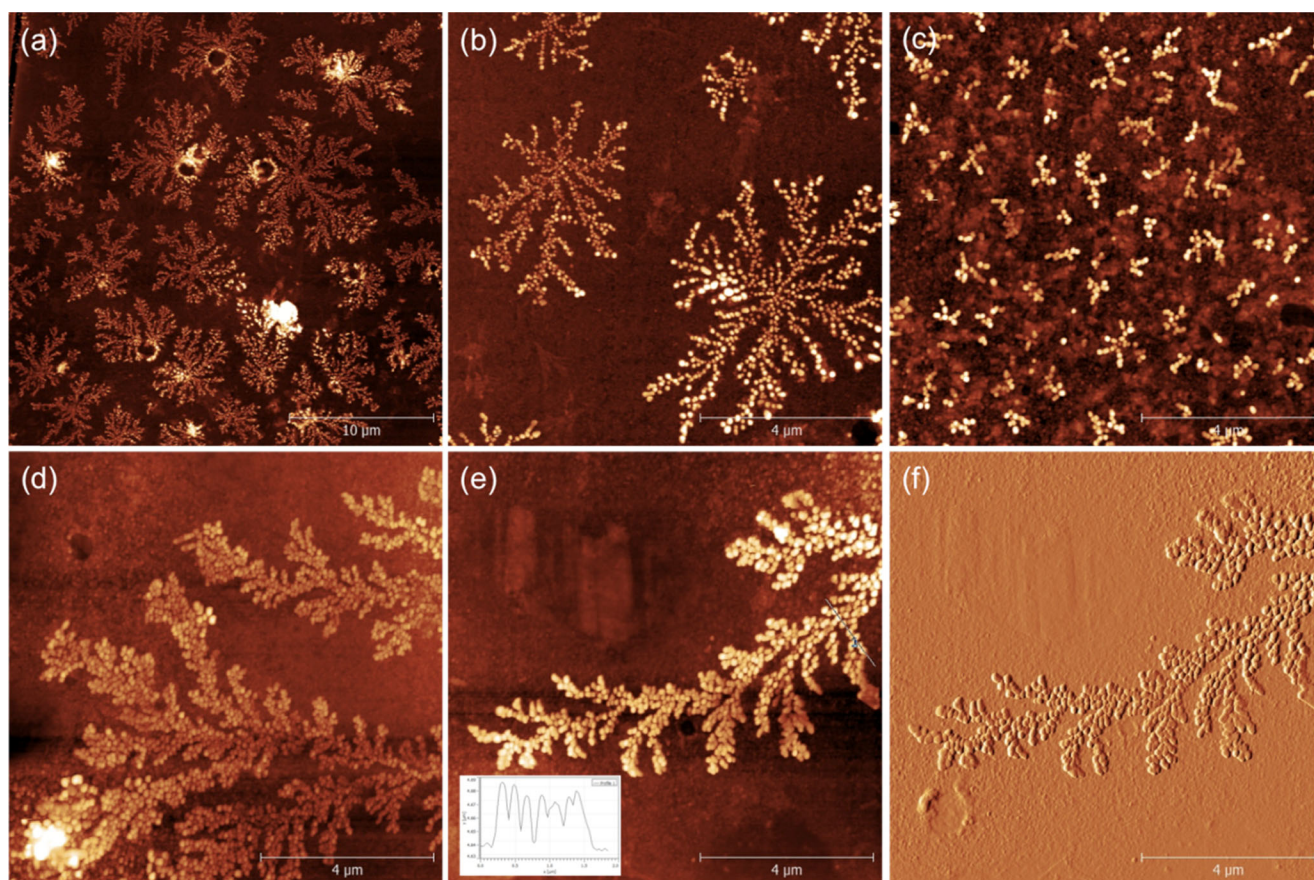
Fig. 2 Height determined using AFM at different magnifications showing the clusters of polymersomes in glass (**a**)-(**e**). The insert on (**e**) show the intensity profile with the high and diameter of the vesicles in a

branch that correspond to the straight line on the figure. (**f**) Show the vertical defection corresponding to (**e**)

protocol was described in a previous paper by Gonzalez-Perez et al. [22]. The polymer concentration used in our experiments was about 10 mg in 1,5 ml of distilled water, and slight changes in the polymer concentration did not result in substantial changes in the pattern after deposition.

After depositing a 1,5 μl drop onto a clean glass surface, we left the sample to dry at room temperature and then investigated the different polymer patterns on the solid support. After the sample was completely dry we obtained different topographic images of the present patterns on the glass using atomic force microscopy in contact mode with an AFM Nanowizard II from JPK.

Figure 1 show a scheme of the drying process. The concentric circles represent the area of contact between the droplet and the glass over specific time frames. During the deposition process (through evaporation); the drying process, droplet size, polymersome concentration and deposited pattern are time-dependent parameters.

With increasing time the droplet area decreases, due to solvent evaporation, following the sequence a > b > c > d where a, b, c and d denotes the corresponding area. Note that the polymersome concentration in the solution changes during the drying process showing increasing concentration at a given time. The precise concentration at each
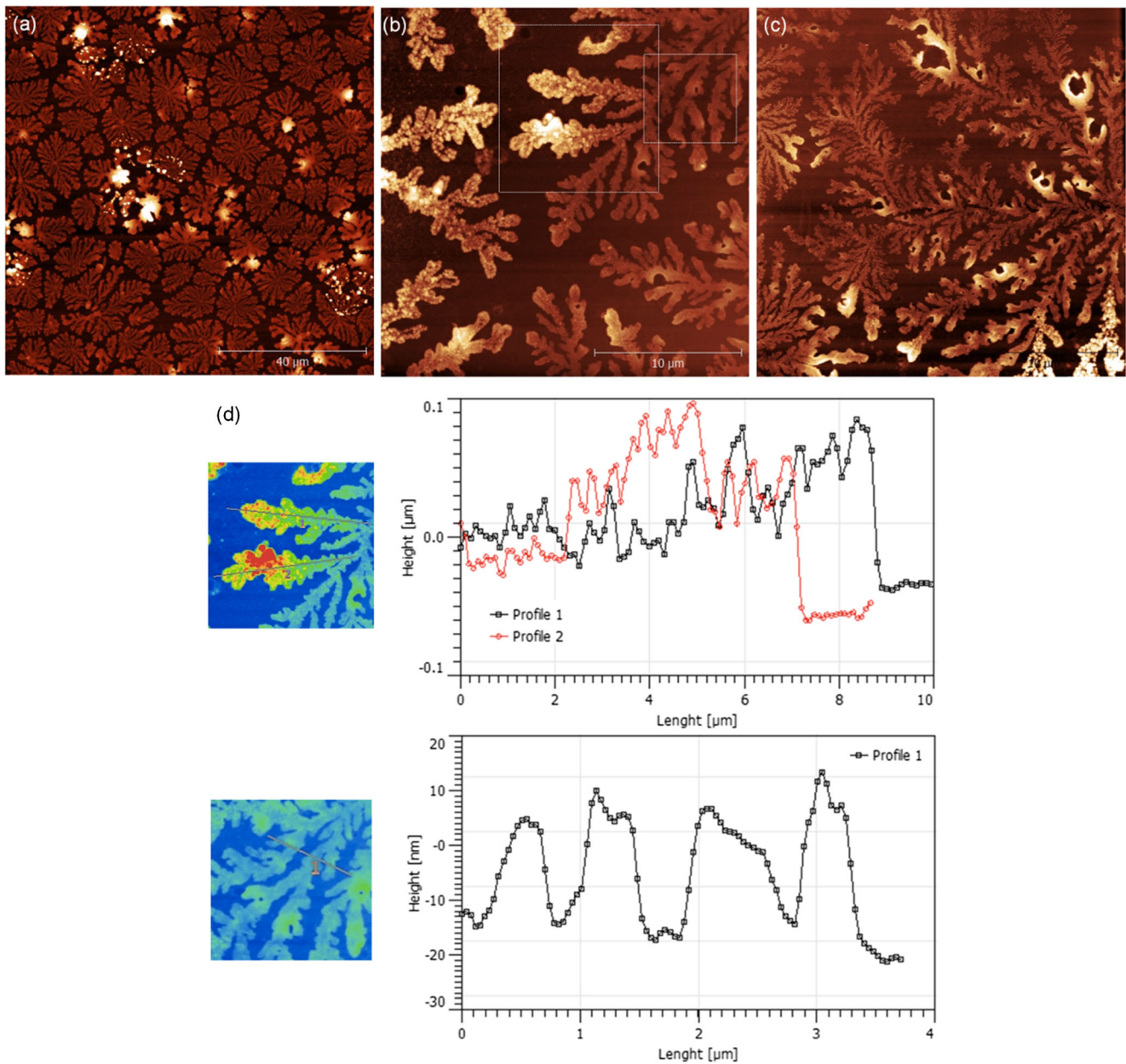
Fig. 3 AFM images with three different colors to enhance the difference in height. On the bottom we show 3 different intensity profiles (corresponding to the lines traced on the selected areas on the left) showing different heights

time is difficult to assess, however it allow us to associate differences in pattern coverage with a qualitative difference in polymersome concentration.

The AFM imaging was performed after the droplet was completely dry looking at different areas within the initial droplet area as shown in the scheme of Fig. 1. We could observe different patterns that appear from the exterior of the starting droplet to the interior. The imaging of such patterns allows us to elucidate the aggregation mechanism. On Fig. 2 we show the formation of clusters of individual vesicles at different magnifications in different regions of the dry sample close to the exterior, (region "a" in Fig. 1). Individual vesicles can be better appreciated at the outermost part of the deposition area (clusters). These areas are defined by the diameter of the deposited droplet where the concentration is lower. However, at the center of the deposition area is more difficult to observe them since there are many more vesicles because the concentration of these increases with deposition time.

Figure 2c corresponds to a nucleation process where the polymersomes start to cluster but the concentration is still low enough to differentiate the individual vesicles. The size of the vesicles in solution was previously determined using dynamic light scattering (DLS) and found to be about 200 nm. A slightly lower size was found, about 180 nm, from the AFM intensity profiles (see Fig. 2e). The differences can be attributed to the dehydration process that results after dry of the sample in the solid support. From (a) to (c) we can observe different stages of the vesicle cluster formation. The branches may grow at distances higher than 10 μm from the same nucleus. Each polymersome cluster keeps their individuality and does not mix with the neighbors. Despite of the short PMOXA hydrophobic chain, with only 7 units, the polymersome adhesion does not result in vesicle fusion and a tree-like pattern, analogous to the one found in bacterial growth under starvation, develops.

We also imaged regions close to the center of the deposition area. After the available area is covered by tree-like structures, in areas where the concentration of polymersomes is high (corresponding to "d" in Fig. 1), the remaining vesicles deposit on top of the branches increasing the density of vesicles and forming different layers. At the end of the branches we can observe that polymersomes can be merged to generate a more uniform layer where the individual vesicles can no longer be identified. The onset of this "fusion" can be seen in Fig. 2f.

On Fig. 3 we show AFM images as an example of fused vesicles within the fractal structure.

After initial fusion of vesicles, the pattern grows in height as we can show in Fig. 3d. We can observe different profiles corresponding to the accumulation of layers of vesicles. Note that the growing in height is not uniform as we can observe in the same patters areas with more or less layers.

To get insight of the nature of the aggregation process and learn about the dynamic of the pattern formation we proceed

to the calculation of the fractal dimension. The fractal dimension is related to the number of vesicles n with the size s of the cluster by $n = s^d$. The fractal dimension is given by using the expression, $d = \frac{ln_n}{ln_s}$, where n is the number of vesicles and s the linear size of the structure. The value of d can be determined by using the box-counting method [24] and is given by the slope of the linear portion of a $\log(N(s))$ versus $\log(1/s)$ graph. Where s represents the different sizes of the square of mesh and $N(s)$ is the number of mesh boxes that contain part of the image. For fractal dimension estimation we developed custom MATLAB codes based on the original algorithm (MATLAB R2012b, MathWorks Inc., Natick, MA, USA). The original images were opened, processed and fractal dimension was evaluated with these programs.

In Fig. 4 we show the log-log graph for different areas imaged in the dry sample, as well as the percentage of the area cover by the polymer as a function of the fractal dimension.
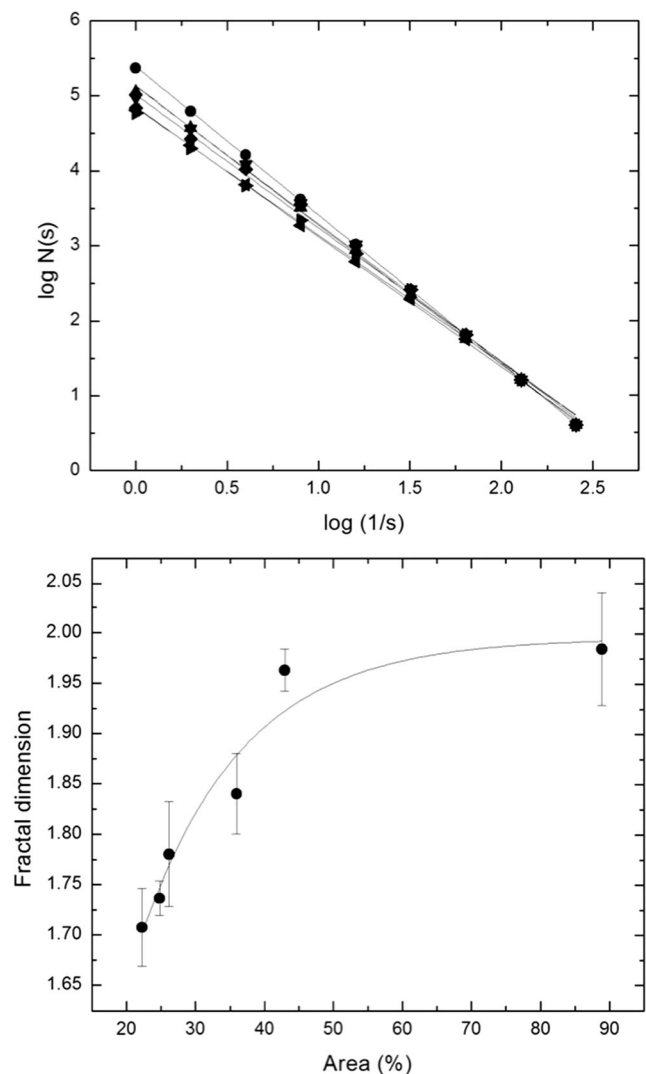
Fig. 4 (*top*) Log-Log plot for different regions imaged. (*bottom*) Fractal dimension versus area covered by the polymersome pattern

The uncertainty in the fractal dimension was estimated using several AFM images at different coverage area.

The fractal dimension at low covered areas corresponds to a diffusion-limited aggregation or DLA process, with values about 1.74 [25, 26] typical for fractal aggregates of particles [27].

Looking at the different areas we can observe that the patterns grow in two directions with successive incorporation of vesicles, at the top and apical region of each existing cluster in an analogous way to growth in some biofilms. An increase of the fractal dimension value that goes asymptotically into Euclidean dimension of 2 can be observed (see Fig. 4). The successive incorporation of vesicles on the top of the cluster contributes to form a compacted layer resulting from fused vesicles. This phenomenon appears in biofilm growth during the maturation process where the cells can fuse and release their interior into a common internal area protected from the external environment.

The AFM imaging in the successive areas from the exterior to the interior of the sampling area can be used as a time frame following different steps in the growth of the fractal pattern. When concentration goes extremely high the pattern become morphologically like a biofilm structure. The result of successive layers of vesicles fused on top of each other increase substantially the available surface area of the artificial biofilm.

In summary, we have showed that by simple spreading-drying of a solution of highly stable polymersomes it is possible to get insights about kinetics of polymersome aggregation onto solid supports. The current work has showed the 2D aggregation of polymersomes in an analogous way to bacterial growth under starvation and demonstrated that this aggregation follows a DLA-like model. The patterns formed show a fractal dimension that change according to the polymersome concentration during the drying process. Additionally, the perpendicular growth increases the surface area in analogy to the process of biofilm grow and maturation.

This method allows the surface functionalization by mimicking the biofilm formation with potential application in biofouling prevention. The structure could be fixed by adding cross-likable methacrylate groups at the PMOXA hydrophobic motif. The outstanding physicochemical properties and biocompatibility of this block copolymer suitable for membrane protein reconstitution can be a valuable tool to develop new nanostructures that mimic fractal patterns in biofilm formation opening new routes for surface modification.

References

1. Hall-Stoodley L, Costerton JW, Stoodley P (2004) Bacterial biofilms: from the Natural environment to infectious diseases. Nat Rev Micro 2(2):95–108
2. Flemming HC, Wingender J, Szewzyk U (2011) Biofilm Highlights. Springer Science & Business Media, Berlin
3. Rudge TJ, Federici F, Steiner PJ, Kan A, Haseloff J (2013) Cell Polarity-Driven Instability Generates Self-Organized, Fractal Patterning of Cell Layers. ACS Synth Biol 2(12):705–714. doi:10.1021/sb400030p
4. Rudge TJ, Steiner PJ, Phillips A, Haseloff J (2012) Computational Modeling of Synthetic Microbial Biofilms. ACS Synth Biol 1(8): 345–352. doi:10.1021/sb300031n
5. Hori K, Matsumoto S (2010) Bacterial adhesion: From mechanism to control. Biochem Eng J 48(3):424–434. doi:10.1016/j.bej.2009.11.014
6. Krishnamoorthy M, Hakobyan S, Ramstedt M, Gautrot JE (2014) Surface-Initiated Polymer Brushes in the Biomedical Field: Applications in Membrane Science, Biosensing, Cell Culture, Regenerative Medicine and Antibacterial Coatings. Chem Rev 114(21):10976–11026. doi:10.1021/cr500252u
7. Kingshott P, Wei J, Bagge-Ravn D, Gadegaard N, Gram L (2003) Covalent Attachment of Poly(ethylene glycol) to Surfaces. Critical for Reducing Bacterial Adhesion Langmuir 19(17):6912–6921. doi:10.1021/la034032m
8. Roosjen A, van der Mei HC, Busscher HJ, Norde W (2004) Microbial Adhesion to Poly(ethylene oxide) Brushes: Influence of Polymer Chain Length and Temperature. Langmuir 20(25):10949–10955. doi:10.1021/la048469l
9. Adams N, Schubert US (2007) Poly(2-oxazolines) in biological and biomedical application contexts. Adv Drug Deliv Rev 59(15): 1504–1520. doi:10.1016/j.addr.2007.08.018
10. Pidhatika B, Rodenstein M, Chen Y, Rakhmatullina E, Mühlebach A, Acikgöz C, et al. (2012) Comparative Stability Studies of Poly(2-methyl-2-oxazoline) and Poly(ethylene glycol) Brush Coatings. Biointerphases 7(1–4):1–15. doi:10.1007/s13758-011-0001-y
11. de la Rosa V (2014) Poly(2-oxazoline)s as materials for biomedical applications. J Mater Sci Mater Med 25(5):1211–1225. doi:10.1007/s10856-013-5034-y
12. Hamley IW (2005) Nanoshells and nanotubes from block copolymers. Soft Matter 1(1):36–43. doi:10.1039/b418226j
13. Hamley IW (2003) Nanotechnology with Soft Materials. Angew Chem Int Ed 42(15):1692–1712. doi:10.1002/anie.200200546
14. Mai Y, Eisenberg A (2012) Self-assembly of block copolymers. Chem Soc Rev 41(18):5969–5985. doi:10.1039/c2cs35115c
15. Kita-Tokarczyk K, Grumelard J, Haefele T, Meier W (2005) Block copolymer vesicles—using concepts from polymer chemistry to mimic biomembranes. Polymer 46(11):3540–3563. doi:10.1016/j.polymer.2005.02.083
16. Zhang X, Tanner P, Graff A, Palivan CG, Meier W (2012) Mimicking the cell membrane with block copolymer membranes. J Polym Sci A Polym Chem 50(12):2293–2318. doi:10.1002/pola.26000
17. Egli S, Schlaad H, Bruns N, Meier W (2011) Functionalization of Block Copolymer Vesicle Surfaces. Polymers 3(1):252
18. Kuang L, Fernandes DA, O'Halloran M, Zheng W, Jiang Y, Ladizhansky V, et al. (2014) "Frozen" Block Copolymer Nanomembranes with Light-Driven Proton Pumping Performance. ACS Nano 8(1):537–545. doi:10.1021/nn4059852
19. Hammer DA, Robbins GP, Haun JB, Lin JJ, Qi W, Smith LA et al. Leuko-polymersomes. Faraday Discuss 2008;139(0):129–141. doi:10.1039/b717821b.

20. Levine DH, Ghoroghchian PP, Freudenberg J, Zhang G, Therien MJ, Greene MI, et al. (2008) Polymersomes: a new multi-functional tool for cancer diagnosis and therapy. Methods (San Diego, CA, United States) 46(1):25–32. doi:10.1016/j.ymeth.2008.05.006

21. Hammer DA, Kamat NP (2012) Towards an artificial cell. FEBS Lett 586(18):2882–2890. doi:10.1016/j.febslet.2012.07.044

22. Gonzalez-Perez A, Castelletto V, Hamley IW, Taboada P (2011) Biomimetic triblock copolymer membranes: from aqueous solutions to solid supports. Soft Matter 7(3):1129–1138. doi:10.1039/c0sm00711k

23. González-Pérez A, Stibius KB, Vissing T, Nielsen CH, Mouritsen OG (2009) Biomimetic triblock copolymer membrane arrays: a stable template for functional membrane proteins. Langmuir 25(18):10447–10450

24. Vicsek T (1992) Fractal Growth Phenomena. World Scientific, Singapore

25. Jullien R (1987) Aggregation phenomena and fractal aggregates. Contemp Phys 28(5):477–493. doi:10.1080/00107518708213736

26. Coffey W, Kalmykov YP (2006) Fractals, Diffusion, and Relaxation in Disordered Complex Systems. Wiley, New York

27. Botet R, Jullien R (1990) Fractal aggregates of particles. Phase Transit 24–26(2):691–736. doi:10.1080/01411599008210249